

## Regular article

# Computation of stationary points via a homotopy method

Stefan Ackermann<sup>1</sup>, Wolfgang Kliesch<sup>2</sup>

<sup>1</sup>Fakultät für Mathematik und Informatik, Universität Leipzig, D-04109 Leipzig, Germany

<sup>2</sup>Max-Planck-Institut für Mathematik in den Naturwissenschaften, Inselstrasse 22-26, D-04103 Leipzig, Germany

Received: 6 May 1996 / Accepted: 2 April 1998 / Published online: 23 June 1998

**Abstract.** A homotopy method is presented that locates both minimizers and saddle points of energy functions in an efficient manner. In contrast to other methods, it makes possible the exploration of large parts of potential energy surfaces. Along a homotopy path stationary points of odd and even order occur alternately. A path tracing procedure requiring only gradients and at most one evaluation of the Hessian matrix is given. Test results on a model potential and three MINDO/3 potentials are reported.

**Key words:** Potential energy surface – Stationary points – Homotopy method – Uphill path

## 1 Introduction

Numerical procedures that locate both minimizers and saddle points of energy functions in an efficient manner are indispensable for the exploration of potential energy surfaces (PESs). Quasi-Newton methods (cf., e.g. [1–3]) locate stationary points very efficiently, provided a good initial guess is available. Unfortunately, often only poor guesses are available, especially for saddle-point searches. Of particular interest are therefore numerical procedures that can scan large parts of PESs in the search for stationary points. Such a procedure is introduced in the present paper. It is based on the homotopy principle, i.e. the principle of continuous deformation; cf. e.g. [4]. Mezey [5] has used this principle to describe reaction mechanisms by classes of homotopic reaction paths. In the present paper the homotopy principle is applied to the gradient of a restriction  $E$  of an energy function  $E_0$  to locate stationary points of  $E_0$ . The homotopy principle cannot be applied to the gradient of  $E_0$  because the stationary points of  $E_0$  are not isolated. Some basic relations between the energy functions  $E$  and  $E_0$  are given in Sect. 2. The graph of  $E_0$ , i.e. the set

$\{(\mathbf{x}, E_0(\mathbf{x})) \mid \mathbf{x} \in \mathbb{R}^{3n}\}$  ( $n \dots$  number of nuclei), is the PES of the molecular system under consideration.

Suppose  $\mathbf{x}_*$  is a stationary point of the restricted energy function  $E$ , which is defined on  $\mathbb{R}^m$ ,  $m = 3n - 6$ . Then  $\mathbf{x}_*$  is a root of the gradient  $g$  of  $E$ , i.e.  $g(\mathbf{x}_*) = 0$ . Thus, the stationary points of  $E$  can be determined by solving the equation

$$g(\mathbf{x}) = \mathbf{0}. \quad (1)$$

Here, to solve Eq. (1), the function  $g$  is embedded in a one-parametric family of continuous functions  $h(\cdot, \rho)$ ,  $\rho \in [0, 1]$  such that  $h(\cdot, 0)$  equals a (trivial) function  $f$  for which a root  $\mathbf{x}_0$  is known, and  $h(\cdot, 1) = g$ , i.e.  $h(\mathbf{x}, 1) = g(\mathbf{x})$  for all  $\mathbf{x} \in \mathbb{R}^m$ . (Recall that the notation  $h(\cdot, \rho)$  means that the parameter  $\rho$  is fixed whereas the first variable varies.) In this way the function  $f$  is continuously deformed to the gradient  $g$  by the homotopy function  $h$ . Under certain conditions, which are discussed in Sect. 3, the solution set of the equation

$$h(\mathbf{x}, \rho) = \mathbf{0} \quad (2)$$

consists of continuous curves (*homotopy paths*) which join a root  $\mathbf{x}_0$  of the function  $f$  and a root  $\mathbf{x}_1$  of the gradient  $g$ . Thus, a solution of Eq. (1) can be determined by tracing a homotopy path of Eq. (2). In Fig. 1 the idea of the homotopy method is illustrated. The graph of the homotopy function  $h$  is a two-dimensional surface over  $\mathbb{R} \times [0, 1] \subset \mathbb{R}^2$ . The boundaries of the surface are defined by the linear function  $f = h(\cdot, 0)$  and the nonlinear function  $g = h(\cdot, 1)$ . The intersection of the graph of  $h$  with the hyperplane  $\mathbb{R}^2$ , which is nothing else than the solution set of Eq. (2), determines a continuous curve which joins the root  $\mathbf{x}_0$  of  $f$  and a root  $\mathbf{x}_1$  of  $g$ . Thus  $\mathbf{x}_1$  can be located by following the homotopy path that originates at  $\mathbf{x}_0$ . For example, the function

$$h(\mathbf{x}, \rho) := g(\mathbf{x}) - (1 - \rho)g(\mathbf{x}_0)$$

is a homotopy function. The point  $\mathbf{x}_0$  is a root of the function  $h(\mathbf{x}, 0) = f(\mathbf{x}) = g(\mathbf{x}) - g(\mathbf{x}_0)$  and  $h(\mathbf{x}, 1) = g(\mathbf{x})$  for all  $\mathbf{x}$  of the domain of  $g$ . In Sect. 4 further homotopy functions appropriate to locate stationary points of energy functions are given.

The most important properties of the homotopy method are the following:

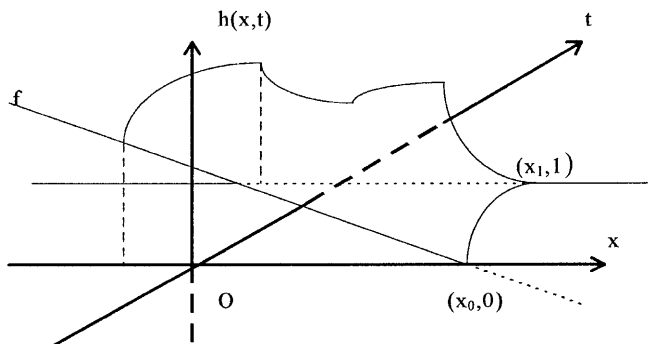


Fig. 1. Homotopy surface and homotopy path

1. The method can be started at an arbitrary point.
2. The type of the stationary point that will be located can be determined a priori.
3. More than one stationary point can be located along a homotopy path.

Property (2) is of particular interest in locating saddle points while property (3) enables scanning of large parts of an energy surface. In Sect. 3 the mathematical background material for the homotopy method is provided. In Sect. 5 a path tracing algorithm is given. Test results are reported in Sect. 6.

## 2 Some background material

The molecular systems considered in the present paper are always constrained in the following manner: One nucleus is fixed at the origin and, after rotation around the origin, another one is only allowed to move along the  $x$ -axis. The motion of a third nucleus is constrained to the  $xy$ -plane. The energy function  $E$  of the constrained molecular system is the restriction of the energy function  $E_0$  of the (unconstrained) molecular system.

The vector of all  $3n$  nuclear coordinates is denoted by  $\hat{x}$  whereas  $x$  denotes the vector that is obtained from  $\hat{x}$  by cancelling six coordinates of  $\hat{x}$ . The gradient and the Hessian matrix of  $E$  at a point  $x$  are denoted by  $g(x)$  and  $H(x)$ , respectively.

The following theorem justifies the computation of stationary points of an energy function  $E_0$  via the described restriction  $E$  of  $E_0$ .

### 2.1 Theorem 1

If  $x_* \in \mathbb{R}^{3n-6}$  is a stationary point of the restriction  $E$  of  $E_0$  then the augmented vector  $\hat{x}_* \in \mathbb{R}^{3n}$  is a stationary point of the unrestricted energy function  $E_0$ .

The theorem can be proven using the fact that the sum and the torque of the gradient forces vanish.

The question arising now is whether a stationary point  $x_*$  of  $E$  and the augmented stationary point  $\hat{x}_*$  of  $E_0$  possess the same order. (Recall that the order of a stationary point is equal to the number of negative eigenvalues of the Hessian matrix at that point.) An answer is given by Theorem 2.

### 2.2 Theorem 2

Suppose  $x_*$  is a regular point of the restricted energy function  $E$ , i.e.  $\det H(x_*) \neq 0$ . If  $x_*$  is a stationary point of order  $k$  of  $E$  then  $\hat{x}_*$  is a stationary point of order  $k$  of the energy function  $E_0$ .

The theorem can be proven by the Sturmian separation theorem [6].

## 3 Homotopy method

In recent years homotopy methods for solving nonlinear equations have extensively been explored [4, 7, 8]. Here only some basic features should be recalled. Suppose  $h: \mathbb{R}^m \times \mathbb{R} \mapsto \mathbb{R}^m$  is a continuously differentiable function that fulfills the following assumptions:

- (A1) There is a point  $u_0 = (x_0, \rho_0) \in \mathbb{R}^m \times \mathbb{R}$  such that  $h(u_0) = \mathbf{0}$ .
- (A2)  $h(\cdot, 1) = g$ .
- (A3) The Jacobian matrix  $h'(u_0)$  has maximal rank, i.e.  $\text{rank } h'(u_0) = m$ .

A point  $u = (x, \rho) \in \mathbb{R}^m \times \mathbb{R}$  is called a *regular point* (*singular point*) of  $h$  if  $\text{rank } h'(u) = m$  ( $\text{rank } h'(u) < m$ ).

### 3.1 Theorem 3

There is a smooth curve  $c: \mathcal{I} \mapsto \mathbb{R}^m \times \mathbb{R}$  for some open interval  $\mathcal{I} = (a, b)$  containing zero such that for all  $\tau \in \mathcal{I}$  [4]:

1.  $c(0) = u_0$ ,
2.  $h(c(\tau)) = \mathbf{0}$ ,
3.  $\text{rank } h'(c(\tau)) = m$ ,
4.  $c'(\tau) \neq \mathbf{0}$ .

Notice that the  $(m, m+1)$ -matrix  $h'(u)$ ,  $u \in \mathbb{R}^m \times \mathbb{R}$ , can be decomposed in the following manner:

$$h'(u) = (h'_x(u) \ h'_\rho(u)), \quad u = (x, \rho), \quad (3)$$

where  $h'_x(u) := \partial h(u) / \partial x$  is an  $(m, m)$ -matrix and  $h'_\rho(u) := \partial h(u) / \partial \rho$  is an  $m$ -vector.

Henceforth the curve  $c(\tau)$  is parametrized with respect to the arc length  $s$ . Differentiation with respect to the arc length is indicated by a dot.

### 3.2 Theorem 4

If  $-\infty < a$  then the curve  $c(s)$  converges to a limit point  $u_{\text{lim}}$  as  $s \rightarrow a$ ,  $s > a$ , which is a singular point of  $h$ . An analogous statement holds if  $b < \infty$  [4].

A solution set of  $h$  is illustrated in Fig. 2. A path tracing started at the point  $u_0$  follows the curve  $c(s)$  until the level  $\rho = 1$  is reached at the point  $u_1 = (x_1, 1)$ . The point  $x_1$  is a stationary point of the energy function  $E$ . If the curve tracing is continued beyond that point, a second solution  $u_2 = (x, 1)$  is located at the level  $\rho = 1$ . The point  $x_2$  is a further stationary point of  $E$ . The curve

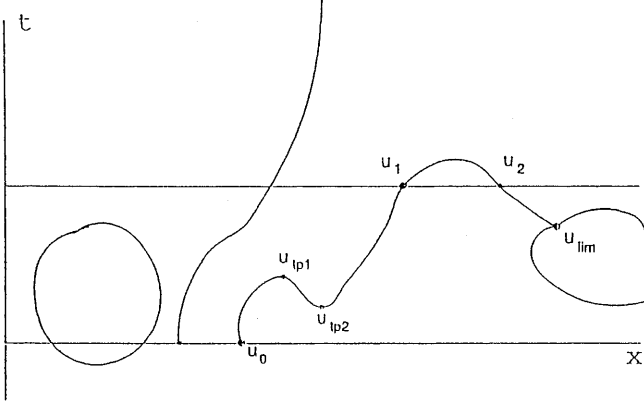


Fig. 2. Set of roots of a homotopy function

terminates at the limit point  $\mathbf{u}_{\text{lim}}$ . The procedure presented in the appendix jumps over such points and continues the curve tracing by following one of the bifurcating curves. A solution curve need not reach the level  $\rho = 1$ . This case, however, occurs very seldom in our experience.

An implicitly defined curve  $\mathbf{c}(s)$  is called *positively (negatively) oriented* if the determinant of the augmented matrix

$$A(s) = \begin{pmatrix} h'(\mathbf{c}(s)) \\ \dot{\mathbf{c}}(s)^\top \end{pmatrix}$$

is positive (negative).

The next theorem underlies almost all path tracing procedures.

### 3.3 Theorem 5

Let  $\mathbf{c}(s)$  be a positively oriented solution curve which satisfies  $\mathbf{c}(0) = \mathbf{u}_0$  and  $h(\mathbf{c}(s)) = \mathbf{0}$  for  $s$  in some open interval  $\mathcal{I}$  containing zero. Then for all  $s \in \mathcal{I}$ , the tangent vector  $\dot{\mathbf{c}}(s)$  satisfies the following conditions [4]:

1.  $h'(\mathbf{c}(s))\dot{\mathbf{c}}(s) = \mathbf{0}$ ;
2.  $\|\dot{\mathbf{c}}(s)\| = 1$ ;
3.  $\det A(s) > 0$ .

If the Jacobian matrix  $h'(\mathbf{u})$  has maximal rank then the system (1–3) possesses one and only one solution. In other words, at each regular point of  $h$  a tangent vector can be defined. Subsequently at a regular point  $\mathbf{u}$  of  $h$  the vector uniquely determined by the conditions (1–3) is called a *tangent vector* and denoted by  $t(h'(\mathbf{u}))$ . At isolated singular points the solution curves of Eq. (2) cross each other, and the system (1–3) does not possess any unique solution. By virtue of Theorems 3 and 5, each solution curve of Eq. (2) satisfies the differential equation

$$\dot{\mathbf{u}} = t(h'(\mathbf{u})). \quad (4)$$

Notice that Eq. (4) is defined only for the regular points of  $h$ . It is easy to verify that

$$h(\mathbf{u}(s)) = \text{const}$$

for each trajectory  $\mathbf{u}(s)$  of Eq. (4). Hence, the trajectory passing through  $\mathbf{u}_0$  belongs to the solution set of Eq. (2). This observation enables us to solve Eq. (2) by integrating Eq. (4). Since the desired trajectory satisfies Eq. (2) and Eq. (4) it can be traced by a predictor-corrector method. This means that first a simple (low cost) integration step, e.g. an Euler step, can be taken and thereafter the approximate curve point is improved by a local equation solver, e.g. a Newton-like method [1–3]. The procedure described in Sect. 5 follows this strategy. Notice that each solution curve  $\mathbf{c}(s)$  of Eq. (2) consists of a *path of configurations*  $\mathbf{x}(s)$  and a parameter curve  $\rho(s)$ . The path of configurations describes a continuous deformation of the initial configuration. At each curve point  $\mathbf{c}(s) = (\mathbf{x}(s), \rho(s))$  the equation

$$\dot{\rho}(s) \det A(s) = \det h'_x(\mathbf{c}(s)) \quad (5)$$

holds [7]. Observe that the matrix  $h'_x(\mathbf{c}(s))$  is singular if and only if  $\dot{\rho}(s) = 0$  or  $\det A(s) = 0$ . A point  $\mathbf{u}_* = \mathbf{c}(s_*)$  is called a *turning point* of the curve  $\mathbf{c}(s)$  if  $\dot{\rho}(s)$  changes the sign at  $s_*$  and  $\det A(s_*) \neq 0$ . Because of Theorem 3 point (3) and Eq. (3)  $\text{rank } h'_x(\mathbf{c}(s)) \geq m - 1$  for all  $s \in \mathcal{I}$ . Thus, by virtue of Eq. (5),  $\text{rank } h'_x(\mathbf{u}_*) = m - 1$  at a turning point  $\mathbf{u}_*$  of the curve  $\mathbf{c}(s)$ . If  $h'_x(\mathbf{u})$  is a symmetric matrix then one and only one eigenvalue of the matrix  $h'_x(\mathbf{u}_*)$  vanishes. If  $\det A(s_*) = 0$ , the point  $\mathbf{u}_* = \mathbf{c}(s_*)$  is called a *bifurcation point* of  $\mathbf{c}(s)$ . By virtue of Theorems 3 and 4 each bifurcation point of  $\mathbf{c}(s)$  is a limit point of  $\mathbf{c}(s)$ . In Fig. 2 the points  $\mathbf{u}_{\text{ip1}}$  and  $\mathbf{u}_{\text{ip2}}$  are turning points whereas the point  $\mathbf{u}_{\text{lim}}$  is a bifurcation point. Suppose the points  $\mathbf{u}_1 = (\mathbf{x}_1, \rho_1)$  and  $\mathbf{u}_2 = (\mathbf{x}_2, \rho_2)$ ,  $\rho_i \in (0, 1)$ , are *strongly joined* by the curve  $\mathbf{c}(s) = (\mathbf{x}(s), \rho(s))$ , i.e.  $\mathbf{c}(s_1) = \mathbf{u}_1$  and  $\mathbf{c}(s_2) = \mathbf{u}_2$ ,  $s_1 < s_2$ , and  $\rho(s) \notin (0, 1)$  for all  $s \in (s_1, s_2)$ . If the matrices  $h'_x(\mathbf{u}_1)$  and  $h'_x(\mathbf{u}_2)$  (cf. Eq. (3)) are regular, then

$$\text{sign } \det h'_x(\mathbf{u}_2) = \begin{cases} \text{sign } \det h'_x(\mathbf{u}_1) & \text{if } \rho_1 \neq \rho_2 \\ -\text{sign } \det h'_x(\mathbf{u}_1) & \text{if } \rho_1 = \rho_2 \end{cases} \quad (6)$$

cf. [9]. In words, if the points  $\mathbf{u}_1$  and  $\mathbf{u}_2$  belong to one and the same level, along the segment of the curve  $\mathbf{c}(s)$  which strongly joins these points an odd number of eigenvalues of the matrix  $h'_x(\mathbf{u})$  changes the sign. If the points  $\mathbf{u}_1$  and  $\mathbf{u}_2$  belong to different levels, an even number of eigenvalues of  $h'_x(\mathbf{u})$  changes the sign (zero is regarded as an even number in this context). Thus by Eq. (6) the type of a stationary point of  $E$  that is located by a path tracing procedure can be determined a priori.

## 4 Homotopy functions

In the present section some homotopy functions appropriate to determine stationary points of an energy function  $E : \mathbb{R}^m \mapsto \mathbb{R}$ , are given and commented upon.

### 4.1 Standard homotopy

$$h(\mathbf{x}, \rho) := g(\mathbf{x}) - (1 - \rho)g(\mathbf{x}_0), \quad \mathbf{x}, \mathbf{x}_0 \in \mathbb{R}^m.$$

Obviously, the point  $\mathbf{u}_0 = (\mathbf{x}_0, 0)$  fulfills assumption (A1). Since  $h(\cdot, 1) = g$ , assumption (A2) is also fulfilled. If  $H(\mathbf{x}_0)$  is regular, the Jacobian matrix

$$h'(\mathbf{u}) = (H(\mathbf{x}) \quad g(\mathbf{x}_0)), \quad \mathbf{u} = (\mathbf{x}, \rho), \quad (7)$$

of  $h$  has maximal rank at  $\mathbf{u}_0 = (\mathbf{x}_0, 0)$  (assumption A3). Conditions which guarantee that a solution curve of the standard homotopy is passing through a solution of Eq. (1) are given in [10]. By differentiating Eq. (2) the equation

$$H(\mathbf{x})\dot{\mathbf{x}} = -\dot{\rho}g(\mathbf{x}_0) \quad (8)$$

is obtained for the standard homotopy. Because along a standard homotopy path

$$g(\mathbf{x}) = (1 - \rho)g(\mathbf{x}_0) \quad , \quad (9)$$

the homotopy method can be regarded as a continuous Newton method if the standard homotopy is employed. For more details see [10].

Suppose the curve  $\mathbf{c}(s) = (\mathbf{x}(s), \rho(s))$  strongly joins the points  $\mathbf{u}_0 = (\mathbf{x}_0, 0)$  and  $\mathbf{u}_1 = (\mathbf{x}_1, 1)$ . Then, by virtue of Eq. (6)

$$\text{sign det } H(\mathbf{x}_1) = \text{sign det } H(\mathbf{x}_0)$$

since  $h'_x(\mathbf{u}) = H(\mathbf{x})$ ,  $\mathbf{u} = (\mathbf{x}, \rho)$ . Particularly, if  $\text{det } H(\mathbf{x}_0) > 0$ , then the point  $\mathbf{x}_1$  is a minimizer or a saddle point of even order of  $E$ . If  $\text{det } H(\mathbf{x}_0) < 0$ , then  $\mathbf{x}_1$  is a saddle point of odd order or a maximizer of  $E$ . If the embedding parameter  $\rho$  is a monotonically increasing function on the interval  $[0, s_1]$ , the matrices  $H(\mathbf{x}_0)$  and  $H(\mathbf{x}_1)$  possess the same numbers of positive and negative eigenvalues because of Eq. (5). Hence, in this case  $\mathbf{x}_1$  is a minimizer of  $E$  if  $H(\mathbf{x}_0)$  is positively definite and a saddle point of first order if  $H(\mathbf{x}_0)$  possesses one and only one negative eigenvalue. The procedure given in Sect. 5 monitors the derivative of the embedding parameter  $\rho$  along the homotopy path. Thus the type of a located stationary point can be determined without evaluating the Hessian matrix, provided the path has not passed through a bifurcation point.

#### 4.2 Convex homotopy

$$h(\mathbf{x}, \rho) := \rho g(\mathbf{x}) + (1 - \rho)M(\mathbf{x} - \mathbf{x}_0), \quad \mathbf{x}, \mathbf{x}_0 \in \mathbb{R}^m \quad .$$

Here  $M$  denotes an arbitrary regular  $(m, m)$ -matrix. Mostly  $M = H(\mathbf{x}_0)$  or  $M = I$  (identity matrix) are chosen. The convex homotopy with  $M = I$  is called *Marquardt homotopy*. It is easy to verify that  $h(\mathbf{x}_0, 0) = \mathbf{0}$  and  $h(\cdot, 1) = g$ . Thus the assumptions (A1) and (A2) are fulfilled. A simple straightforward calculation shows that

$$h'(\mathbf{u}) = (\rho H(\mathbf{x}) + (1 - \rho)M \quad g(\mathbf{x}) - M(\mathbf{x} - \mathbf{x}_0)), \quad (10)$$

$$\mathbf{u} = (\mathbf{x}, \rho) \quad .$$

Thus in the case of the Marquardt homotopy ( $M = I$ ), the initial guess  $\mathbf{u}_0 = (\mathbf{x}_0, 0)$  is always a regular point of  $h$ . If  $M = H(\mathbf{x}_0)$ ,  $\mathbf{u}_0$  is a regular point of  $h$  if  $H(\mathbf{x}_0)$  is a regular matrix. If the initial guess  $\mathbf{u}_0 = (\mathbf{x}_0, 0)$  and a solution point  $\mathbf{u}_1 = (\mathbf{x}_1, 1)$  are strongly joined by a homotopy path, the equality

$$\text{sign det } H(\mathbf{x}_1) = \text{sign det } M$$

holds (cf. Eqs. 6 and 10). Hence, in the case of the Marquardt homotopy a path tracing always provides a minimizer first. If the path is followed beyond that point a saddle point can be found (cf. Eq. 6). If  $M = H(\mathbf{x}_0)$  is chosen the stationary point encountered first is determined by the sign of the Hessian matrix at the starting point.

#### 4.3 $d$ -trick homotopy [11]

$$h(\mathbf{x}, \rho) := g(\mathbf{x}) - (1 - \rho)\mathbf{d}, \quad \mathbf{x}, \mathbf{d} \in \mathbb{R}^m, \mathbf{d} \neq \mathbf{0} \quad .$$

If a solution of Eq. (1) is known, an additional solution can be computed by the  $\mathbf{d}$ -trick homotopy. The choice of the vector  $\mathbf{d}$  is not restricted in any way. The assumptions (A1)–(A3) are fulfilled if  $\mathbf{x}_0$  is a stationary point of  $E$  at which the Hessian matrix of  $E$  is regular. Also in the case of the  $\mathbf{d}$ -trick homotopy the homotopy method can be regarded as a continuous Newton method ( $g(\mathbf{x}_0)$  has to be reset by  $\mathbf{d}$  in Eq. 8). The Jacobian matrix is given by

$$h'(\mathbf{u}) = (H(\mathbf{x}) \quad \mathbf{d}) \quad . \quad (11)$$

Conditions which ensure that the  $\mathbf{d}$ -trick homotopy locates additional solutions are discussed in [11]. Notice that after passing through the hyperplane  $\rho = 1$  a standard homotopy path coincides with the  $\mathbf{d}$ -trick homotopy path,  $\mathbf{d} = g(\mathbf{x}_0)$ . The vector  $\mathbf{d}$  determines the direction along which the path of configurations leaves the stationary point. This follows from the equation

$$H(\mathbf{x})\dot{\mathbf{x}} = -\dot{\rho}\mathbf{d} \quad (12)$$

which is obtained by differentiating the equation

$$g(\mathbf{x}) - (1 - \rho)\mathbf{d} = \mathbf{0} \quad . \quad (13)$$

Thus the  $\mathbf{d}$ -trick homotopy enables the searches to start in a prescribed direction. In particular, if  $\mathbf{d}$ ,  $\|\mathbf{d}\| = 1$ , is an eigenvector of the Hessian matrix  $H(\mathbf{x}_0)$ , then

$$\begin{pmatrix} \dot{\mathbf{x}}(0) \\ \dot{\rho}(0) \end{pmatrix} = \frac{1}{\sqrt{1 + \lambda^2}} \begin{pmatrix} -\mathbf{d} \\ \lambda \end{pmatrix}$$

where  $\lambda$  denotes the eigenvalue which belongs to  $\mathbf{d}$ . Hence the path of configuration leaves the initial point along one of the directions of principal curvature. Suppose  $\mathbf{x}_1$  is a minimizer of  $E$  and the curve  $\mathbf{c}(s)$  strongly joins the points  $\mathbf{u}_1 = (\mathbf{x}_1, 1)$  and  $\mathbf{u}_2 = (\mathbf{x}_2, 1)$ . Then, because of Eq. (6),  $\mathbf{x}_2$  is a saddle point of odd order of  $E$ . Therefore, in this situation the path tracing method can be regarded as an uphill walking method. In contrast to the walking methods by Cerjan and Miller [12] and Nichols et al. [13] the homotopy method does not require the computation of any eigenvector. Observe that the curve  $\mathbf{c}(s)$  possesses one turning point at least (Fig. 1). If  $\mathbf{u}_{tp}$  is the first turning point which is encountered along  $\mathbf{c}(s) = (\mathbf{x}(s), \rho(s))$ , then  $\mathbf{u}_{tp}$  is just the point at which the curve  $\mathbf{x}(s)$  leaves the educt region (more popular “educt valley”) and enters the saddle point region. Here educt region means the largest

neighbourhood of  $x_1$  on which the energy function  $E$  is convex.

## 5 A path tracing procedure

The following predictor-corrector scheme is used to follow a homotopy path numerically (see Fig. 3): If  $\mathbf{u}$  is an arbitrary point of a solution curve  $\mathbf{c}(s)$ , first an Euler step of length  $\tau$  along the tangent vector  $t(h'(\mathbf{u}))$  is taken, i.e.

$$\mathbf{v} := \mathbf{u} + \tau t(h'(\mathbf{u})) . \quad (14)$$

Thereafter the predictor  $\mathbf{v}$  is corrected toward the solution curve by a Newton step, i.e.

$$\mathbf{w} := \mathbf{v} - h'(\mathbf{v})^\dagger h(\mathbf{v}) .$$

Here  $h'(\mathbf{v})^\dagger$  denotes the Moore-Penrose inverse of  $h'(\mathbf{v})$ ; see step 3 of procedure PATH in the appendix. The point  $\mathbf{w}$  is an approximate solution to the minimization problem [4]

$$\min_{\mathbf{z}} \{ \|\mathbf{z} - \mathbf{v}\| \mid h(\mathbf{z}) = \mathbf{0} \} .$$

The time-consuming evaluations of the Jacobian matrix  $h'(\mathbf{u})$  are avoided by Georg's generalized Broyden update method [4]. The tangent vectors are also updated [4] such that no linear equation needs to be solved. The details are given in the appendix. For the step size control an algorithm by Rheinboldt and Burkhardt [14] has been adapted. The step size is always chosen so that the predictor points are situated within a certain vicinity of the solution curve. More precisely, in some vicinity of a curve point  $\mathbf{u}_i$  the curve  $\mathbf{c}(s)$  is approximated by the quadratic Hermite-Birkhoff interpolating polynomial

$$\mathbf{p}(\delta) = \mathbf{u}_i + \delta t(h'(\mathbf{u}_i)) + \frac{\delta^2}{2} \mathbf{q}_i ,$$

where

$$\mathbf{q}_i = \frac{t(h'(\mathbf{u}_i)) - t(h'(\mathbf{u}_{i-1}))}{\Delta \mathbf{u}_i} , \quad \Delta \mathbf{u}_i = \mathbf{u}_i - \mathbf{u}_{i-1} .$$

It is easy to verify that

$$\mathbf{p}(0) = \mathbf{u}_i, \quad \mathbf{p}'(0) = t(h'(\mathbf{u}_i)), \quad \mathbf{p}'(-\mathbf{u}_i) = t(h'(\mathbf{u}_{i-1})) .$$

The equation

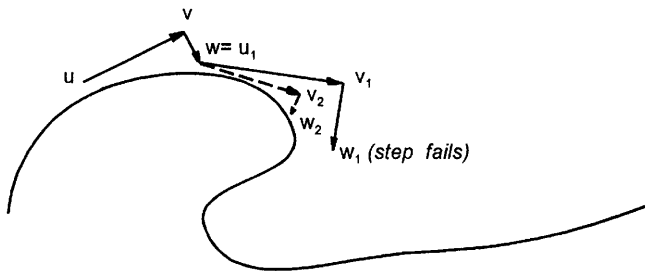


Fig. 3. Predictor-corrector method:  $\mathbf{u}_1$  and  $\mathbf{w}_2$  are accepted corrector points whereas  $\mathbf{w}_1$  is a rejected corrector (see procedure PATH)

$$\|\mathbf{p}(\delta) - \mathbf{u}_{i+1}(\delta)\| = \frac{\delta^2}{2} \mathbf{q}_i$$

gives an estimate of the distance between the tangent line (see Eq. 14) and the solution curve  $\mathbf{c}(s)$ . Hence, if a difference that is equal to a given tolerance  $\varepsilon > 0$  at most is accepted, then a step length

$$\tau_{i+1} = \sqrt{\frac{2\varepsilon}{\|\mathbf{q}_i\|}}$$

should be chosen.

Procedure PATH which is given in the appendix requires to evaluate the Hessian matrix at the starting point at most. The gradient has to be computed twice in each cycle. The walking method [12, 13, 15] needs one gradient and the direction of ascent (or descent) per cycle. Since the direction of ascent (descent) is determined by an eigenvector of the Hessian matrix, the numerical effort of the walking method will be higher than that of the homotopy method if the Hessian matrix is evaluated in each cycle. If the Hessian matrix is updated, per cycle the numerical effort of the walking method will be less than that of the homotopy method. In this case, however, there is no guarantee that the updated matrix and the Hessian matrix possess the same numbers of negative and positive eigenvalues, especially in the vicinity of a saddle point [3]. The essential advantage of the homotopy method is that a well-defined curve is followed which leads to a stationary point with probability one. Only the differential equation methods [16, 17] possess a similar property. But, the trajectories may meander in some vicinity of a stationary solution. Moreover the homotopy method provides information about the stationary point a priori. The procedure PATH is included in the TURBO-PASCAL program package EYRING [18] which uses a MINDO/3-energy function [19]. An  $\alpha$ -version of the program package can be obtained from the authors on request.

## 6 Test results

Some results of an extensive testing are presented subsequently. Note that convex homotopy always means that  $M = H(\mathbf{x}_0)$  has been chosen; cf. Sect. 4. The Hessian matrices have been computed numerically.

### 6.1 Müller-Brown potential

First the procedure PATH has been tested on the Müller-Brown potential which is defined in [20]. The results obtained by means of the standard, convex and Marquardt homotopy are given in Table 1. To show that the homotopy method works globally an initial guess  $\mathbf{x}_0$  has been chosen that will hardly belong to the domain of attraction of an iterative root finding method. By standard and convex homotopy all known stationary points were located along *one* path. The solutions have been refined to an accuracy of  $\|g(\mathbf{x})\| < 10^{-4}$ . The curves of configurations are plotted in Figs. 4 and 5. Observe that minimizers and saddle points alternate along the

curves, just as the theory says; see Sect. 3. By the Marquardt homotopy only one minimizer was discovered. The search for further stationary points stopped as the embedding parameter exceeded the limit  $\rho_{\max}$ . Thus the Marquardt homotopy comes out worst in the testing because: (1) it has located only one minimizer and (2) it needed significantly more predictor-corrector steps than the two other homotopies to locate this point.

When the  $\mathbf{d}$ -trick homotopy is employed to locate additional stationary points the  $\mathbf{d}$ -vector should be chosen very carefully, because numerical problems can occur if  $\mathbf{d}$  equals an eigenvector of the Hessian matrix. At a solution point  $\mathbf{u} = (\mathbf{x}, \rho)$  of Eq. (13) the tangent vector  $t(h'(\mathbf{u})) = (\dot{\mathbf{x}}^\top, \dot{\rho})^\top$  fulfills Eq. (12). If  $(\mathbf{d}, \lambda)$  is

an eigenpair of  $H(\mathbf{x})$ , then  $t(h'(\mathbf{u})) = \alpha(\mathbf{d}^\top, \lambda)^\top$  with  $|\alpha| = (\|\mathbf{d}\|^2 + \lambda^2)^{-1/2}$ . Now, if  $\lambda$  is very large in magnitude, the Euclidean norm of the vector  $\alpha\mathbf{d}$  becomes very small and  $|\alpha\lambda| \approx 1$ . Hence the changes in the coordinate vector  $\mathbf{x}$  are very small (they may even become insignificant) whereas the changes in the embedding parameter are very large. In such a situation the path tracing procedure becomes numerically unstable and the number of predictor-corrector steps increases rapidly. Such numerical instabilities can be avoided by choosing  $\mathbf{d}$  so that the components of  $\mathbf{d}$  are of about the same magnitude as the corresponding eigenvalue. All that is convincingly demonstrated by the results given in Table 2. Different  $\mathbf{d}$ -vectors need not lead to different stationary points, even if the  $\mathbf{d}$ -vectors are eigenvectors; see Table 2 and Fig. 6. On the other hand, by using one and the same  $\mathbf{d}$ -vector different stationary points may be located if the homotopy path is traced in both directions.

Observe that the path tracings started at the minimizer  $\mathbf{m}_2$ , end at the saddle point  $s_1$  or  $s_2$  (see Table 2 and Fig. 6). The path tracings started at the saddle point  $s_1$ , end at the minimizer  $\mathbf{m}_1$  or  $\mathbf{m}_2$ . Thus the procedure PATH can be employed as both an uphill and a downhill procedure.

**Table 1.** Müller-Brown potential. Results of homotopy path tracings started at  $(1.0, 0.0)^\top$

Solution <sup>a</sup>	PC-steps		
	Standard homotopy	Convex homotopy	Marquardt homotopy
$\mathbf{m}_1$	15	28	80
$s_1$	67	63	–
$\mathbf{m}_2$	43	47	–
$s_2$	37	43	–
$\mathbf{m}_3$	167	92	–
<i>total</i>	329	273	

<sup>a</sup> See Fig. 4

## 6.2 Hydrocyanic-acid MINDO/3-PES

The HCN/CNH rearrangement is often used to test saddle-point search procedures. Independently of the

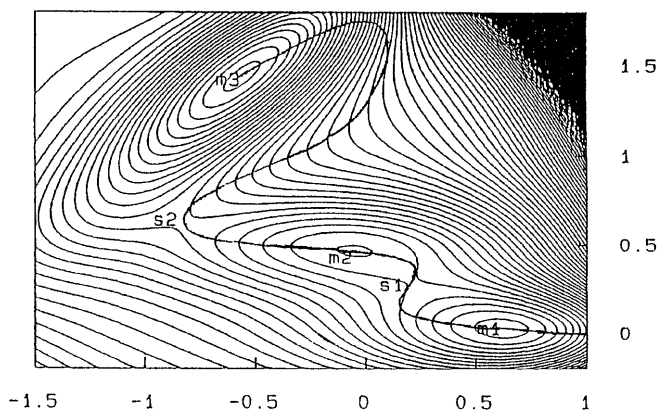


**Fig. 4.** Müller-Brown potential. Curve of configurations of the standard homotopy path (cf. Table 1)

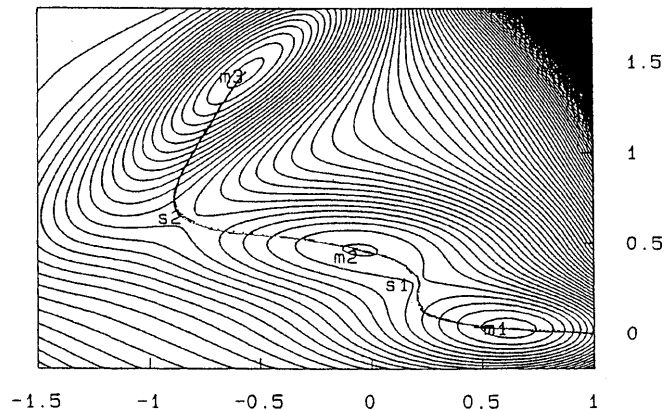


**Fig. 5.** Müller-Brown potential. Curve of configurations of the convex homotopy path (cf. Table 1)

**Table 2.** Müller-Brown potential. Results of  $\mathbf{d}$ -trick homotopy path tracings

Initial data			Results		
Point <sup>a</sup>	$\mathbf{d}$ -vector <sup>b</sup>	<i>DIR</i> <sup>c</sup>	Solution <sup>a</sup>	PC-steps	$\rho_{\max}^c$
$\mathbf{m}_2$	$\mathbf{v}_1$	1	$s_1$	1266	48.71
$\mathbf{m}_2$	$10 \mathbf{v}_1$	1	$s_1$	255	5.77
$\mathbf{m}_2$	$10^2 \mathbf{v}_1$	1	$s_1$	67	1.48
$\mathbf{m}_2$	$10^3 \mathbf{v}_1$	1	$s_1$	32	1.05
$\mathbf{m}_2$	$10^3 \mathbf{v}_2$	1	$s_1$	36	
$\mathbf{m}_2$	$10^3 \mathbf{v}_1$	–1	$s_2$	45	
$\mathbf{m}_2$	$10^3 \mathbf{v}_2$	–1	$s_2$	74	
$s_1$	$\mathbf{v}_2$	1	$\mathbf{m}_2$	29	
$s_1$	$\mathbf{v}_2$	–1	$\mathbf{m}_1$	69	

<sup>a</sup> cf. Fig. 4

<sup>b</sup>  $\mathbf{v}_i$  denotes  $i$ -th eigenvector of the Hessian matrix at the initial point

<sup>c</sup> See procedure PATH in appendix

choice of the energy function about 8–10 gradient calls are needed in general to determine the transition structure of the HCN/CNH isomerization [16, 17, 21]. Using the standard homotopy five cycles ( $\approx 10$  gradient calls) were needed to locate the saddle point (starting configuration [17]:  $r(\text{HC}) = 1.211 \text{ \AA}$ ,  $r(\text{CN}) = 1.182 \text{ \AA}$ ,  $\angle(\text{HCN}) = 71.3^\circ$ ). Thus the homotopy method does not work less efficiently than other methods in this case.

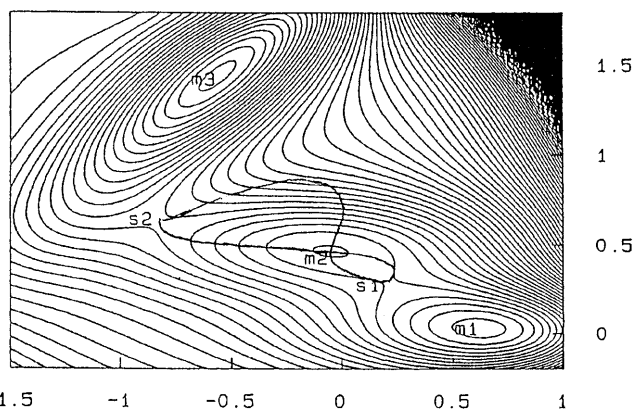


**Fig. 6.** Müller-Brown potential. Curves of configurations of the  $d$ -trick homotopy paths (cf. Table 2)

**Table 3.** Formaldehyde MINDO/3-potential energy surface PES. Initial configurations

	$x_1$			$x_2$		
C	0.0	0.0	0.0	0.0	0.0	0.0
O	1.2	0.0	0.0	1.2	0.0	0.0
H	-1.0	0.6	0.0	-1.0	0.5	0.0
H	1.0	0.0	0.0	-0.5	1.4	0.0

### 6.3 Formaldehyde MINDO/3-PES

Using the initial guesses given in Table 3 and the minimizer  $m$  (see Fig. 7) stationary-point searches have been carried out. The results are summarized in Table 4. For all solutions the Euclidean norm of the gradient is smaller than  $2.5 \times 10^{-5}$ . Since the numerical effort necessary to locate a stationary point is determined above all by the total number of predictor-corrector (PC) steps and the evaluation of the Jacobian matrix at the starting point (cf. Eqs. 7–11), the total number of gradient calls ( $\#g$ ) has been chosen as a measure of the numerical effort. Particularly, each PC-step requires two gradient calls, while an approximation to the reduced Hessian matrix requires  $2(3n - 6)$  gradient calls (central differences). Although the Marquardt homotopy does not require any evaluation of the Hessian matrix (see Eq. 10), the procedure PATH is not less efficient when the standard homotopy is used; see Table 4. Procedure PATH started at guess  $(x_2, 0)$  failed when the Marquardt homotopy was used. The standard homotopy locates two stationary points where the second stationary point is of even order (in this case a minimizer) just as the theory says; cf. Eq. (6).

The  $d$ -trick homotopy started at the minimizer  $m$  needed considerably more steps than the standard or the convex homotopy to locate the saddle point  $s_1$ . The main reason is that the distance between the configurations  $m$  and  $s_1$  is considerably larger ( $\|m - s_1\| = 1.36 \text{ \AA}$ ) than that between  $x_2$  and  $s_1$  ( $\|x_2 - s_1\| = 0.22 \text{ \AA}$ ). The saddle point  $s_2$  could be localized only by the  $d$ -trick homotopy. The walking method proposed by Cerjan and Miller needed 11 cycles (at STO-2G level) to step from the formaldehyde minimizer  $m$  to the transition structure  $s_1$  [12]. However, the numerical effort per cycle is considerably larger for the employed walking method than for the homotopy method because in each cycle a finite difference approximation to the Hessian matrix was computed. It should be stressed here once more that the

**Fig. 7.**  $\text{H}_2\text{CO}$ -system

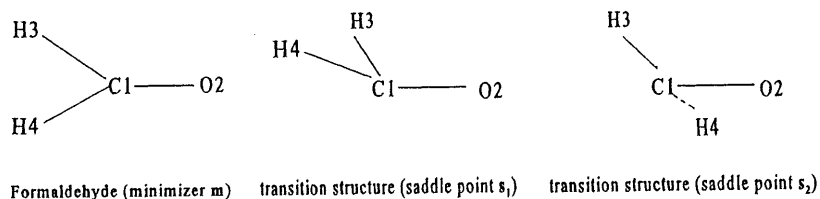


**Table 4.** Formaldehyde MINDO/3-PES. Results of path tracings

Homotopy	Initial data			Results		
	Guess <sup>a</sup>	$d$ -vector <sup>b</sup>	DIR <sup>c</sup>	Solution <sup>d</sup>	PC-steps	$\#g$ <sup>e</sup>
Standard	$x_1$			$m$	23	58
	$x_2$			$s_1$	12	36
				$m$	124	248
Convex	$x_1$			$m$	27	66
	$x_2$			$s_1$	15	42
Marquardt $d$ -trick	$x_1$			$m$	28	56
	$m$	$d_1$	1	$s_1$	130	272
	$m$	$d_1$	-1	$s_2$	96	204
	$m$	$d_2$	1	$s_2$	54	120

<sup>a</sup> See Table 3 and Fig. 7

<sup>b</sup>  $d_1 = 6^{-1/2}(1, \dots, 1)^T$ ,  $d_2$  equals the reduced lowest frequency mode

<sup>c</sup> See procedure PATH in appendix

<sup>d</sup> See Fig. 7

<sup>e</sup> See text

essential advantage of the homotopy method is that it follows a well-defined path which leads to a stationary point with probability one. Saddle-point searches normally require a large number of trial and error optimizations which easily may require a large computational effort. Therefore, if the *total* computational efforts are compared, the homotopy method is an efficient tool to locate stationary points.

#### 6.4 Ethyl cation MINDO/3-PES

Searches for stationary points have been carried out using the initial guesses given in Table 5. The solutions have been refined to an accuracy of  $5 \times 10^{-5}$ . The test results summarized in Table 6 confirm the results above: (1) procedure PATH is an efficient tool to locate stationary points of energy functions, (2) using the standard homotopy the procedure is most efficient, (3) using the Marquardt homotopy saddle points can only be detected after passing through a minimizer.

### 7 Summary

The homotopy method is an efficient tool to explore large parts of PESs. Especially, if only poor guesses are

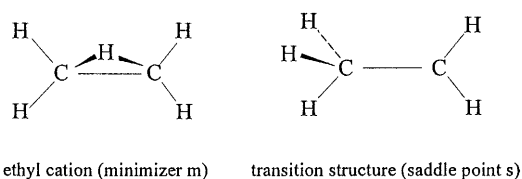


Fig. 8.  $C_2H_5^+$ -System

available, the homotopy method locates both minimizer and saddle points in an efficient manner. More than one stationary point can be discovered along a homotopy path, where stationary points of odd and even order occur alternately. The standard homotopy should be preferred in general. If only minimizers are desired the Marquardt homotopy should be chosen. If a stationary point is known, additional stationary points can be determined by means of the *d*-trick homotopy. If this homotopy is used, a path tracing started at a minimizer always leads to a saddle point.

*Acknowledgements.* The authors wish to thank Dr. H. Herrler for assistance in preparing the plots. One author (W.K.) thanks the Deutsche Forschungsgemeinschaft Bonn (Germany) for a grant.

### Appendix

#### Procedure PATH

##### Notations

$\mathbf{x}, \mathbf{y}, \mathbf{z}$ : points of  $\mathbb{R}^{3n-6}$   
 $\mathbf{u}, \mathbf{v}, \mathbf{w}$ : points of  $\mathbb{R}^{3n-6} \times \mathbb{R}$ , i.e.  $\mathbf{u} = (\mathbf{x}, \rho)$ ,  $\mathbf{v} = (\mathbf{y}, \rho)$ ,  
 $\mathbf{w} = (\mathbf{x}, \rho)$  etc.

Input (default values in parentheses)

$\mathbf{x}_0$		initial guess
$\tau_0$	(0.05)	initial step size
$\tau_{\max}$	(0.1)	maximal step size
$\tau_{\min}$	( $1.0^{-6}$ )	minimal step size
$\beta$	(0.5)	reduction factor for step size control
$\kappa_{\max}$	(0.4)	maximal Newton contraction
$\delta_{\max}$	(0.2)	maximal distance to zero

Table 5. Ethyl cation MINDO/3-PES. Initial configurations

	$\mathbf{x}_1$		$\mathbf{x}_2$			$\mathbf{x}_3$			
C	0.0	0.0	0.0	0.0	0.0	0.0	0.0	0.0	0.0
C	1.4	0.0	0.0	1.4	0.0	0.0	1.4	0.0	0.0
H	-0.6	0.0	1.0	-0.5	-1.0	0.0	-0.5	-1.0	0.0
H	0.6	1.0	0.0	-0.5	0.5	1.0	0.5	0.0	1.0
H	2.0	0.0	-1.0	2.0	1.0	0.0	2.0	1.0	0.0
H	2.0	0.0	1.0	2.0	-1.0	0.0	2.0	-1.0	0.0
H	-0.6	0.0	-1.0	0.0	0.5	-1.0	-0.5	1.0	0.0

Table 6. Ethyl cation MINDO/3-PES. Results of path tracings

Homotopy	Initial data		Results		
	Guess <sup>a</sup>	<i>d</i> -vector	Solution <sup>b</sup>	PC-steps	#g <sup>c</sup>
Standard	$\mathbf{x}_1$		<i>m</i>	12	54
	$\mathbf{x}_2$		<i>s</i>	41	112
Convex	$\mathbf{x}_1$		<i>m</i>	14	58
	$\mathbf{x}_2$		<i>s</i>	53	141
Marquardt	$\mathbf{x}_1$		<i>m</i>	29	58
	$\mathbf{x}_2$		<i>m</i>	126	252
	$\mathbf{x}_3$		<i>m</i>	45	120
<i>d</i> -trick	<i>m</i>		<i>s</i>	148	296
	<i>m</i>	$15^{-1/2}(1, \dots, 1)^T$	<i>s</i>	180	
	<i>m</i>	reduced mode to lowest frequency	<i>s</i>	245	

<sup>a</sup> See Table 5 and Fig. 8

<sup>b</sup> See Fig. 8

<sup>c</sup> See text



$\delta_{\min}$	$(1.0^{-5})$	minimal distance to zero
$\alpha_{\max}$	$(12^\circ)$	maximal angle between new and old tangent vectors
$\rho_{\max}$	(50)	maximal value of the embedding parameter
$\varepsilon_1$	$(10^{-3})$	maximal predictor error
$\varepsilon_2$	$(10^{-5})$	stopping error for path tracing
$\varepsilon_3$	$(1.5 \cdot 10^{-6})$	stopping error for quasi-Newton iterations
$FMax$	(10)	maximal number of subsequently rejected steps
$\gamma_{itr}$	(5)	maximal angle between vectors $\mathbf{a}$ and $\mathbf{b}$ (see step 7)
$Dir$	(1)	path tracing direction (1 or -1)

## 1. Initialization

$$\mathbf{u} := (\mathbf{x}_0, 0), \quad \tau := \tau_0, \quad B := h'(\mathbf{u}) \text{ (cf. Eqs. (7)–(11)).}$$

2. Compute the initial tangent  $t(B)$  from the equations  $At(B) = \mathbf{0}$ ,  $\|t(B)\| = 1$ ,  $\text{sign det}(A^T t(B)) = Dir$  (see Theorem 5).

## 3. Determine the Moore-Penrose inverse

$$B^\dagger := B^T(BB^T)^{-1}.$$

## 4. Predictor step

$$\mathbf{v} := \mathbf{u} + \tau t(B).$$

## 5. Corrector step

$$\mathbf{w} := \mathbf{v} - B^\dagger(h(\mathbf{v}) - \mathbf{p}), \quad \|h(\mathbf{v}) - \mathbf{p}\| \geq \delta_{\min}.$$

## 6. Update step

$$\mathbf{a}_* := B^\dagger(h(\mathbf{v}) - \mathbf{p}),$$

$$\mathbf{a} := \mathbf{a}_* / \|\mathbf{a}_*\|,$$

$$\mathbf{b} := B^\dagger(h(\mathbf{w}) - \mathbf{p}) / \|\mathbf{a}_*\|,$$

$$\vartheta := 1 - \mathbf{a}^T \mathbf{b},$$

$$B^\dagger := \left( I + \frac{\mathbf{b}\mathbf{a}^T}{\vartheta} \right) B^\dagger$$

$$\mathbf{t} := \text{sign}(\vartheta) \frac{t(B) - B^\dagger(h(\mathbf{v}) - h(\mathbf{u}))}{\|t(B) - B^\dagger(h(\mathbf{v}) - h(\mathbf{u}))\|},$$

$$B^\dagger := (I - t(B)t(B)^T)B^\dagger.$$

## 7. Compute the control quantities

$$\alpha := \arccos(t(B), \mathbf{t})$$

(angle between old and new tangent vector),

$$\delta := \|h(\mathbf{w}) - \mathbf{p}\|$$

(distance to zero),

$$\gamma := \arccos(\mathbf{a}, \mathbf{b} / \|\mathbf{b}\|)$$

(angle between Newton steps  $\mathbf{a}$  and  $\mathbf{b}$ ),

$$\kappa := \|\mathbf{b}\|$$

(Newton contraction).

## 8. Step size control

if  $|\tau - 1| < \varepsilon_2$  then goto step 9

if  $(\alpha < \alpha_{\max}) \wedge (\delta < \delta_{\max}) \wedge (\kappa < \kappa_{\max})$  then

$$fails := 0$$

$$\tau := \min \left( \sqrt{\frac{2\varepsilon_1 \|\mathbf{u} - \mathbf{w}\|}{\|\mathbf{t} - t(B)\|}}, \tau_{\max} \right)$$

$$\mathbf{u} := \mathbf{w}$$

$$t(B) := \mathbf{t}$$

else

$$fails := fails + 1$$

$$t(B) := \mathbf{t}$$

$$\tau := \max(\beta\tau, \tau_{\min})$$

if  $(\rho + \tau t(B)_{3n-5} > 1)$  then  $\tau := (1 - \rho) / t(B)_{3n-5}$

if  $(fails > FMax)$  then exit

else go to step 4.

## 9. Final iteration

if  $\gamma < \gamma_{itr}$  then

– save the vectors  $\mathbf{u}$  and  $t(B)$  and the Moore-Penrose inverse  $B^\dagger$ ,

– improve  $\mathbf{u}$  by the iteration  $\mathbf{u}_{i+1} = \mathbf{u}_i - B^\dagger h(\mathbf{u}_i)$ .

## 10. Continuation

if the curve tracing is to be continued then

reproduce  $\mathbf{u}, t(B)$  and  $B^\dagger$  and go to step 4

else stop.

## Remarks

1. The direction parameter  $Dir$  does not coincide with the orientation of the solution curve (cf. Sect. 3).  $Dir = 1(-1)$  means that the solution curve is followed so that the embedding parameter  $\rho$  is an increasing (decreasing) function along the curve, at least at the beginning.

2. Vector  $\mathbf{p}$  in steps 5 and 6 improves the numerical stability of the corrector step. It is chosen so that the norm of  $\mathbf{a}_*$  can never become too small to compute the vectors  $\mathbf{a}$  and  $\mathbf{b}$ .

3. In step 8 a point  $\mathbf{u}$  is accepted as an approximate curve point if:

- the angle  $\alpha$  between the old and new tangent is not too large (a small change in  $\mathbf{u}$  should imply a small change in the tangent vector),
- the Newton contraction  $\|\mathbf{b}\|$ , i.e. the quotient of the length of the second and the first Newton corrector, is not too large and
- the value of the homotopy function differs from zero only within a prescribed tolerance.

4. The control quantity  $\gamma$  is the angle between the first and the second Newton direction. It is only of interest for the execution of step 9. If  $\gamma$  is sufficiently small some quasi-Newton steps are performed to improve the accuracy of the located stationary point. But, the larger  $\gamma$ , the farther the iterates can run away from the target hyperplane  $\rho = 1$ . Therefore a quasi-Newton iteration is not carried out if  $\gamma$  exceeds some limit angle  $\gamma_{itr}$ .

5. If the embedding parameter  $\rho$  is greater than 1 in the corrector step, the step is repeated with a smaller step size such that the predictor step just reaches the level  $\tau = 1$ . This is the last instruction in the “then” part of step 8.

6. If the number of subsequently rejected steps exceeds a given number  $FMax$  often the curve tracing procedure cannot pass through a bifurcation point. In this situation the procedure should be restarted.

**References**

1. Fletcher R (1980) Practical methods of optimization: unconstrained optimization. vol 1, Wiley, New York
2. Dennis JĒ Jr, Schnabel RB (1983) Numerical methods for unconstrained optimization and nonlinear equations. Prentice Hall, Englewood Cliffs, N.J.
3. Heidrich D, Kliesch W, Quapp W (1991) Properties of chemically interesting potential energy surfaces. Springer, Berlin
4. Allgower EL, Georg K (1990) Numerical continuation methods. Springer, New York
5. Mezey PG (1987) Potential energy hypersurfaces. Elsevier, Amsterdam
6. Bellmann R (1970) Introduction to matrix analysis. McGraw-Hill, New York
7. Allgower EL, Georg K (1980) SIAM Rev 22:28
8. Watson LT (1989) Appl Math Comp 31:369
9. Garcia CB, Zangwill WI (1979) Math Oper Res 4:390
10. Garcia CB, Gould FJ (1980) SIAM Rev 22:263
11. Allgower EL, Georg K (1980) In: Forster W (ed) Numerical solution of highly nonlinear problems. North-Holland, Amsterdam, p 253
12. Cerjan CJ, Miller WH (1981) J Chem Phys 75:2800
13. Nichols J, Taylor H, Schmidt P, Simons J (1990) J Chem Phys 92:340
14. Rheinboldt WC, Burkhardt JV (1983) ACM Trans Math Softw 9:215
15. Baker J (1986) J Comp Chem 7:385
16. Smith CM (1988) Theor Chim Acta 74:85
17. Kliesch W, Schenk K, Heidrich D, Dachsel H (1988) J Comp Chem 9:810
18. Ackermann S, Berndt W, Herrler HJ, Kliesch W (1994) EYRING: a program package to analyse a MINDO/3-PES. Universität Leipzig, Germany
19. Bingham RC, Dewar MJS, Lo DH (1975) J Amer Chem Soc 97:1285
20. Müller K, Brown LD (1979) Theor Chim Acta 53:75
21. Bell S, Crighton JS (1984) J Chem Phys 80:2464